Noncontact Coil-Type Textile Sensor for Monitoring Cerebral Blood Flow Signals

Jinhee Yang
Institute of Symbiotic Life-TECH, Yonsei University

Hyunseung Cho

https://doi.org/10.5109/7395545

出版情報：Proceedings of International Exchange and Innovation Conference on Engineering & Sciences (IEICES). 11, pp.383-389, 2025-10-30. International Exchange and Innovation Conference on Engineering & Sciences
バージョン：

Noncontact Coil-Type Textile Sensor for Monitoring Cerebral Blood Flow Signals

Jinhee Yang[1], Hyunseung Cho[1]
[1]Institute of Symbiotic Life-TECH, Yonsei University
hyunseung-cho@yonsei.ac.krl

Abstract: *This study proposes a time-varying system-based noncontact coil-type textile sensor for cerebral blood flow (CBF) monitoring and emotion evaluation. The sensor was fabricated by embroidering thirty 40-denier silver threads into a spiral coil structure. For experimental validation, the sensor was attached to the carotid artery, and concurrent measurements of ECG, respiration, and Doppler ultrasound-based blood-flow velocity were performed. Participants viewed emotionally manipulated visual stimuli using Meta Quest 2 and completed an emotion evaluation questionnaire. Results demonstrated that the sensor signal varied consistently with Doppler-measured CBF velocity, verifying its sensitivity to hemodynamic changes. Heart rate variability (HRV) indices extracted from both ECG and textile sensor signals (via PLL) exhibited similar trends in autonomic nervous system responses to visual stimuli. These findings confirm the feasibility of noninvasive, wearable inductive sensing for monitoring cerebral blood flow and emotional states.*

Keywords: Cerebral Blood Flow Monitoring; Noncontact Inductive Sensing; Coil-Type Textile Sensor; Wearable Biosensor; Emotion Evaluation

1. INTRODUCTION

Emotion recognition using physiological signals has long been a subject of interest in affective computing and human-centered research. Traditionally, most studies have relied on controlled laboratory environments, where participants are equipped with multiple wired physiological measurement devices to monitor changes in brain activity (EEG) or cardiac responses (ECG) in reaction to externally presented stimuli. While physiological responses are largely involuntary and thus considered objective indicators of emotion, such laboratory-based setups impose constraints that hinder the natural expression of human affect. Moreover, because emotional states do not shift instantaneously, capturing genuine emotional responses in short, stimulus-driven trials poses a significant methodological challenge. To overcome these limitations, the present study aims to develop a wearable system capable of monitoring physiological signals unobtrusively and noninvasively in real-life settings. By designing a wearable platform that employs non-contact textile electrodes integrated into ordinary clothing, physiological signals can be collected without interfering with the user's daily activities. This approach allows for the real-time acquisition of emotional data in ecologically valid conditions, potentially improving the accuracy and relevance of emotion recognition systems.
However, research on emotion recognition using unconstrained, real-life wearable sensing systems remains extremely limited. Among various physiological indicators, brain hemodynamics and cardiac activity play pivotal roles in the emotional information processing pathway. Previous studies have identified characteristic changes in these signals corresponding to emotional valence: for instance, increased heart rate and elevated EEG beta waves are typically observed during states of excitement or joy, while decreased heart activity and increased alpha waves are associated with calmness or sadness. While extensive research has explored emotion recognition using single modalities such as EEG or ECG, relatively few studies have adopted a multimodal approach integrating diverse physiological signals. Emotions such as surprise or fear stimulate the autonomic nervous system, triggering measurable physiological changes. For example, heart rate variability (HRV), derived from photoplethysmographic signals, has been shown to reflect sympathetic and parasympathetic nervous system dynamics in response to emotional stimuli [1, 2]. Sympathetic activation during stress correlates with faster heart rates, while calm states are linked to slower rhythms [3]. Brain signals also serve as a key component in emotion classification: δ-waves are dominant during sleep, θ-waves during concentration, α-waves during relaxation, β-waves in anxious states, and γ-waves under high arousal or tension [4-5]. Studies such as Cha et al. (2010) have further demonstrated that the use of multiple biosignals—including EEG, ECG, and PPG—improves emotion recognition accuracy over single-signal approaches [6]. While basic affective states (e.g., valence, arousal) can be inferred from physiological signals such as cardiac, cerebral, and respiratory activity [6-11], there is a lack of research addressing the correlation between higher-order emotions—such as curiosity, interest, or aesthetic appreciation—and physiological responses. This gap highlights the need for a more nuanced, multidimensional approach to affective state monitoring.
The ultimate objective of this study is to design a wearable platform system that utilizes non-contact, time-varying magnetic field-based inductive textile sensors to measure multimodal biosignals under natural, unconstrained conditions. Specifically, the study proposes an integrated "biosignal-emotion index" for emotion recognition, using cardiac, respiratory, and cerebral hemodynamic signals. As a foundational step, this research focuses on developing an inductive sensor capable of detecting brain hemodynamic signals via magnetic permeability-based conductivity measurement and exploring its feasibility for real-time emotion monitoring in everyday environments.

Table 1. Measurement of inductance of electrodes

Inductance [H] / Frequency [Hz]	Electrode A (Spiral loop shape / 20strands)	Electrode B (Spiral loop shape / 30strands)	Electrode C (Extrusion loop shape / 20strands)	Electrode D (Extrusion loop shape / 30strands)
	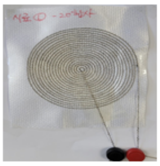	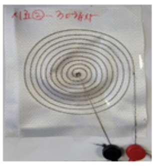	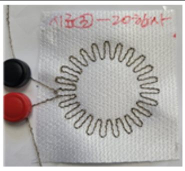	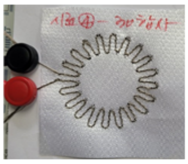
500.0k	 11.275μH	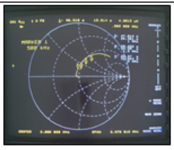 4.3015μH	 670.19nH	 649.21nH
1M	 11.841μH	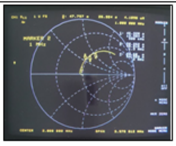 4.1896μH	 524.87nH	 518.96nH
1.5M	 12.146μH	 4.2522μH	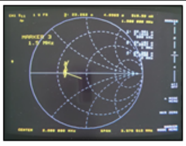 519.53nH	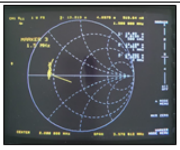 519.64nH
2.0M	 12.7μH	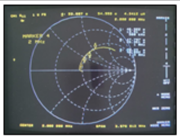 4.3412μH	 513.91nH	 513.87nH
Mean (1.5MHz, 2.0MHz)	12.423μH	4.2967μH	516.144nH	516.755nH

2. MATERIALS AND METHODS

2.1 Instruments

2.1.1 Design of the Coil-Type Textile Sensor

The textile sensor was fabricated by computer embroidery using conductive silver thread (40 denier), implemented in various configurations. In previous studies [12-17], a noncontact, fiber-based capacitive inductive sensor structure was developed to detect cardiac activity (10 × 10 cm, 10 turns). Building on these findings, this study designed both a spiral loop sensor—whose sensing performance had been validated in prior work—and a modified version referred to as the extrusion loop sensor.

Based on these designs, a total of four types of inductive sensors were developed by varying the number of turns (10 turns, 20 turns) and using two different types of conductive silver threads: 20-strand (45 Ω/m) and 30-strand (34 Ω/m) configurations.

Inductance measurements of the electrodes were conducted using a Network Analyzer (8753D, Hewlett Packard), which supports a frequency range from 30 kHz to 6 GHz. During testing, transparent tape was applied to areas where the conductive threads overlapped to prevent direct electrical contact (Fig. 1a). To eliminate measurement error caused by cable movement, the measurement cable was fixed in place (Fig. 1b), and its connection point was secured on paper (Fig. 1c) to ensure consistent positioning.

The frequency range for inductance measurement was set between 1.5 MHz and 2.0 MHz, and the average inductance was calculated across this range. The measured inductance values for each sensor configuration are presented in Table 1.

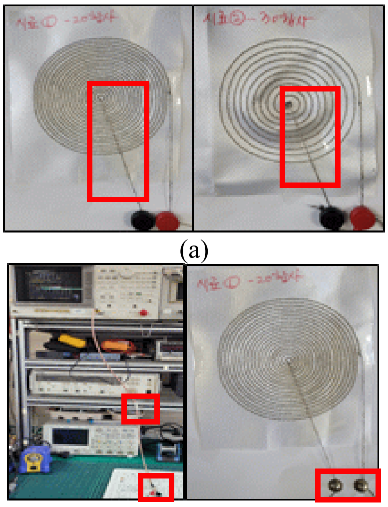

(a)

(b) (c)

Fig. 1. Method for measuring the inductance of coil electrodes: (a) Application of transparent insulating tape, (b) Stabilization of measurement cables, (c) Connection of electrodes to the measurement interface.

2.1.2 Design of the Textile Sensor for Cerebral Blood Flow Signal Detection

To develop a noncontact textile sensor based on a time-varying magnetic field that is robust to motion artifacts and suitable for detecting cerebral blood flow signals with improved signal accuracy, the spiral loop configuration (30-strand silver thread) was selected from the four previously developed textile sensor types, due to its higher inductance characteristics. Although reducing the number of coil turns lowers the inductance, the sensor was miniaturized to 3 × 3 cm to enable attachment to the carotid artery region. To prevent electrical contact between conductive threads within the 3 cm space, the coil was constructed with a total of six turns.

Furthermore, the inductance of the textile sensor was measured within the frequency range of 1.5–3.0 MHz to evaluate its sensing performance (Fig. 2).

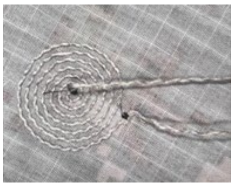

Frequency	Inductance
@1.5MHz	925.35nH
@2.0MHz	925.94nH
@2.5MHz	919.93nH
@3.0MHz	916.95nH

Fig. 2. Coil-type electrode for cerebral blood flow detection and frequency-dependent inductance characteristics

2.1.3 Principle of Cerebral Blood Flow Signal Detection and Design of the Measurement Module

When an alternating current is applied to the coil-shaped textile electrode composed of conductive threads, a time-varying magnetic field is generated according to Equation (1), which in turn induces a change in the electric field. When biological tissue is positioned in close proximity to the sensor, a time-varying current is induced within the tissue in proportion to its conductivity, as described by Faraday's law of induction (Equation (2)). This induced current, along with the resulting electric field, influences the magnetic field, as expressed in Equation (3).

$$\nabla \times E = -\frac{\partial B}{\partial t} \quad (1)$$

$$J = \sigma E \quad (2)$$

$$\nabla \times H = J + \frac{\partial}{\partial t}\epsilon E \quad (3)$$

Here, σ denotes the electrical conductivity of the target material, E is the electric field, H is the magnetic field, B is the magnetic flux density, J is the current density, and D represents the electric displacement (related to permittivity). The eddy currents induced within the target are proportional to the distribution of electrical conductivity along the current path [18-19]. Variations in the internal composition of biological tissues cause changes in impedance, which in turn affect the magnitude of the induced current or voltage. This induced current generates a secondary magnetic field, which—according to Lenz's law—opposes the primary magnetic field that created it (Fig. 3).

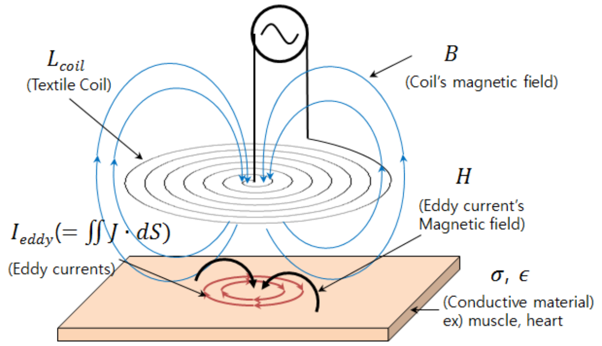

Fig. 3. Mechanism of eddy current induction and its magnetic field interaction [12]

As a result, the induced magnetic flux can be considered as leakage flux depending on the arrangement of the coil, and variations in the inductance of the coil caused by this flux can be interpreted as impedance changes (Equation (4)) [20].

$$\Delta Z_{coil} \approx -\omega^2 \cdot L_{coil} \cdot \Delta I_{eddy} \quad (4)$$

The sensor, when connected to a Colpitts oscillator, modulates the frequency due to changes in inductance caused by blood volume variation. This frequency shift is converted to voltage using a PLL (Phase-Locked Loop), filtered, and output as a CBF signal (Fig. 4).

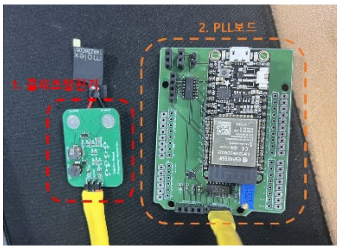

Fig. 4. Circuit module for signal acquisition using a Colpitts oscillator and PLL board

Accordingly, a sensor connected to a Colpitts oscillator is positioned at a site suitable for cerebral blood flow (CBF) measurement. When an alternating current is applied, the magnetic field generated by the coil rapidly fluctuates, inducing eddy currents in the adjacent biological tissue according to Faraday's law. These eddy currents generate a secondary magnetic field, which influences the coil's inductance and consequently alters the oscillation frequency of the Colpitts oscillator.

As changes in blood flow cause fluctuations in vascular volume, the induced eddy currents vary accordingly, leading to changes in the sensor's inductance. This variation in inductance results in a shift in the oscillator's frequency, reflecting the dynamics of cerebral blood flow. The output signal from the Colpitts oscillator is then passed through a phase-locked loop (PLL), which converts the frequency variation into a voltage signal. After filtering, the final cerebral blood flow signal is obtained.

As shown in Fig. 4, the experimental module consists primarily of two components: the Colpitts oscillator and the PLL board. The oscillator is built around an LC tank circuit comprising an inductor (L) and a capacitor (C), where the oscillation frequency is determined by the component values. In this setup, the time-varying magnetic field affects the inductance (L) of the sensor, thereby generating a signal with a modulated frequency. The PLL board converts this frequency shift into a voltage change, allowing for digital processing of the biosignal.

2.1.4 Development of Emotion Evaluation Questionnaire

Traditional emotion research has primarily focused on identifying discrete emotional states based on facial expressions—commonly referred to as the six basic emotions: fear, sadness, happiness, anger, contempt, and surprise. It is well established that when individuals are presented with emotionally intense stimuli (e.g., photographs), the amygdala—a brain region central to emotion regulation—is activated.

More recently, research in cognitive neuroscience has emphasized understanding the influence of emotion on human decision-making. One line of prior work has investigated the effect of emotional stimuli on memory. For example, participants were shown emotionally arousing images (e.g., scenes of blood, firearms, conflict) and neutral images (e.g., houses, landscapes, nature) during an fMRI session. When asked to recall the images one year later, participants demonstrated significantly better memory for the emotionally arousing images compared to the neutral ones. Neuroimaging results confirmed that the amygdala, associated with emotional processing, and the medial temporal lobe, associated with long-term memory retrieval, were more strongly activated in response to the emotionally intense stimuli. These findings suggest that experiences involving strong emotions—such as joy, sadness, or anger—are more likely to be vividly remembered than emotionally neutral events.

Based on this theoretical foundation, the present study selected fear-related items for the emotional evaluation questionnaire. These were adapted from the work of Dillard and Anderson (2004) [21], including statements such as “I feel terrified,” “I feel afraid,” and “I feel scared.” Additional items were drawn from the Beck Anxiety Inventory (BAI) [22], such as “I feel excited,” “I feel restless,” “I feel nervous,” and “I feel anxious.” The items were rated using a five-point Likert scale.

2.1.5 Development of Emotional Stimuli

Emotionally distinctive virtual reality (VR) stimuli were developed by selecting scenes that could elicit clearly differentiated affective responses. Candidate videos included both fear-inducing (e.g., startling or suspenseful scenes) and calming (e.g., healing nature walks) content. These videos were initially shown to five participants, and emotional evaluation results were used to finalize the stimuli for the main experiment.

As a result, three VR videos were selected: one designed to elicit high-intensity fear, one with moderate fear-inducing content, and a control video featuring a relaxing walk through a forest path for comparison. During exposure to these VR stimuli, participants’ cerebral blood flow (CBF), heart activity (ECG), and respiration signals were measured simultaneously. These measurements were used to assess the effectiveness of each stimulus in evoking different levels of emotional arousal, particularly fear (see Fig. 5).

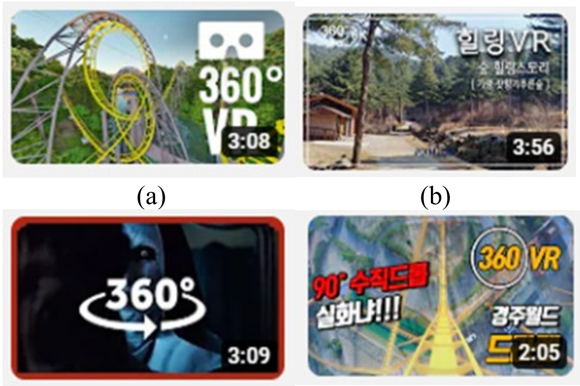

(a) (b) (c) (d)

Fig. 5. Representative VR stimuli for emotional elicitation: (a) Roller coaster, (b) Forest walk, (c) Ghost scene, (d) Racing coaster

2.2 Experimental Method

For the cerebral blood flow (CBF) measurement experiment, a textile electrode (sensor) was attached to the carotid artery region as illustrated in Figs. 6 and 7. In addition, ECG electrodes and a respiration (RSP) measurement belt (BIOPAC system) were applied to monitor cardiac and respiratory activity. An ultrasound diagnostic device (HM70 EVO, Samsung Healthcare Global) was used to position a Doppler probe directly above the textile sensor (Fig. 7a), allowing simultaneous acquisition of blood flow signals from both the textile sensor and the Doppler ultrasound system.

Doppler ultrasonography was performed to measure the velocity of blood flow in the carotid artery. As shown in Fig. 7b, participants wore a Meta Quest 2 headset and were presented with emotion-inducing visual stimuli. While viewing the stimuli, their physiological responses—specifically blood flow changes—were recorded, and participants subsequently completed an emotion evaluation questionnaire.

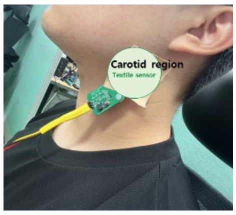

Fig. 6. Localization of the embroidered coil sensor on the neck

(a) (b)

Fig. 7. Experimental setup for multimodal biosignal acquisition: (a) Positioning of ECG and respiration (RSP) electrodes, (b) Attachment of the textile sensor and ECG electrodes, application of RSP belt, and viewing of VR stimuli via Meta Quest 2

3. RESULTS AND DISCUSSION

3.1 Pilot Test for Cerebral Blood Flow Signal Detection

In this study, we conducted a pilot test to verify whether the signal acquired from a time-varying magnetic field-based coil-type textile sensor would vary in accordance with changes in blood flow velocity measured via Doppler ultrasonography. The results confirmed that fluctuations in the blood flow signal measured by the ultrasound probe were reflected in the output of the textile sensor. Specifically, the textile sensor was able to detect blood flow dynamics at the carotid artery site—corresponding to the same region examined by Doppler ultrasound—producing signals such as those shown in Figs. 8 and 9.

The pilot experiment involved three participants (two males and one female in their twenties). As illustrated in Figs. 8 and 9, side-by-side comparisons of simultaneously recorded signals from the same individual demonstrated a clear correspondence between the Doppler-measured blood flow velocity and the signal acquired from the textile sensor. These findings provide preliminary evidence that the proposed coil-type textile sensor is capable of detecting cerebral blood flow activity in a noncontact manner.

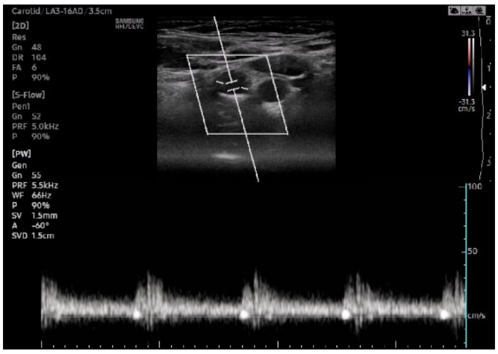

Fig. 8. Doppler ultrasound-derived hemodynamic signals

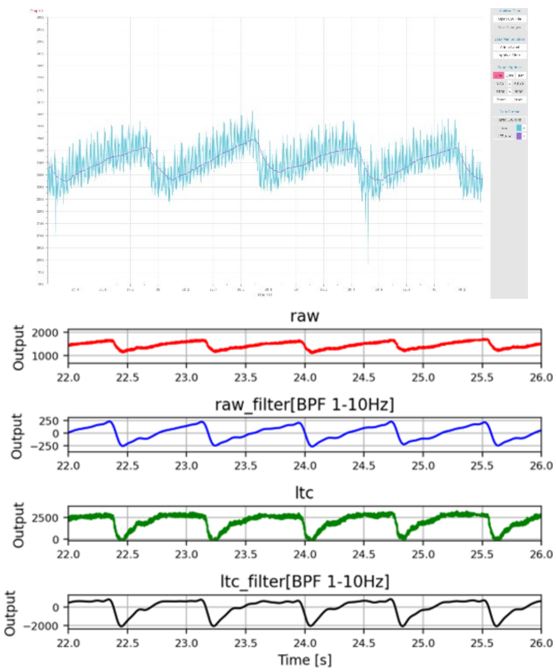

Fig. 9. Inductive biosignal responses measured by time-varying system textile electrodes

3.1 Emotional Evaluation

To examine the correlation between the cerebral blood flow (CBF) signals acquired via the time-varying magnetic field-based coil-type textile sensor (PLL signal) and the ECG and respiration (RSP) signals measured using the BIOPAC system, all three signals—PLL, ECG (lead II), and RSP—were recorded concurrently during the presentation of visual emotional stimuli.

Figure 10 displays the signals obtained from female participant A. The PLL signal was bandpass filtered between 1–10 Hz to remove noise and enhance physiological relevance. As shown in Fig. 10, the signal pattern detected by the textile sensor closely correlates with the ECG waveform, demonstrating a strong temporal alignment.

These results suggest that the textile sensor developed in this study is capable of reliably detecting cerebral blood flow signals, offering promising applicability for affective state monitoring in future wearable biosensing platforms.

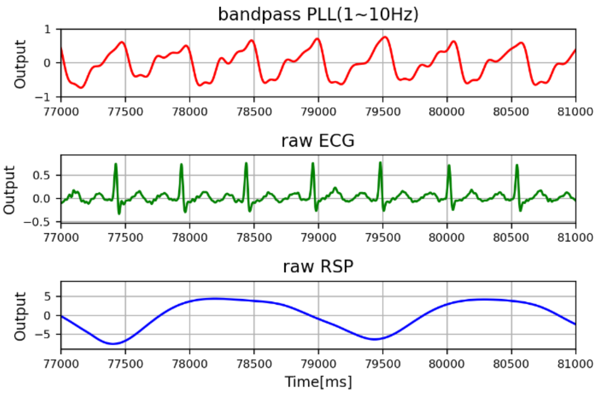

Fig. 10. Simultaneously recorded signals from textile sensor (PLL), ECG (lead II), and respiration (RSP)

In this study, synchronization between the Doppler ultrasound system—used as an integrated diagnostic platform—and the coil-type textile sensor was technically limited. Therefore, emotional state evaluation based on visual stimuli was conducted indirectly through analysis of heart rate variability (HRV), which reflects autonomic nervous system (ANS) activity. HRV refers to the variation in time intervals between successive heartbeats and is a widely recognized indicator of the balance between sympathetic (excitatory) and parasympathetic (inhibitory) nervous system responses, which operate involuntarily.

Psychophysiological tension associated with emotional states such as fear or surprise can be inferred from ANS activity. Activation of the sympathetic nervous system (SNS) manifests through physiological responses such as increased heart rate, vasoconstriction, and respiratory modulation. Accordingly, HRV was extracted using R-R intervals from the ECG signals and peak-to-peak intervals from the textile sensor (PLL signals), which exhibited periodic peak patterns. These results were compared with emotion evaluation questionnaire scores to investigate the feasibility of emotion estimation using textile-sensor-derived signals.

HRV was analyzed using both time-domain and frequency-domain approaches. In this study, frequency-domain analysis was employed, focusing on the lowfrequency (LF) and high-frequency (HF) components. The LF component is associated with sympathetic activity, while the HF component is considered an index of parasympathetic activity. The LF/HF ratio, therefore, serves as a useful marker for determining the relative activation levels of the two branches of the ANS.

Figs. 11 and 12, and Tables 2 and 3, present the HRV results obtained from both ECG and textile (PLL) signals during visual stimulation corresponding to two distinct emotional states. The stimuli were rated by participants using an affective evaluation scale ranging from 0 (no fear) to 28 (maximum fear). In the condition rated as 0 (emotionally calm), the LF/HF ratios were 0.64579 for ECG and 0.321256 for the textile sensor, indicating a dominance of parasympathetic activity. In contrast, during the stimulus rated as 28 (high fear), the LF/HF ratios increased to 1.538189 (ECG) and 1.265557 (textile sensor), reflecting elevated sympathetic activity.

Although some discrepancies were observed between the absolute LF/HF ratios calculated from ECG and PLL signals, both signals demonstrated a consistent trend in autonomic nervous system modulation in response to emotional stimuli. Notably, the PLL signal lacked clearly defined R-peaks like those in ECG, and was more susceptible to noise-induced artifacts, which may have introduced some variance. Nevertheless, the textile sensor produced HRV patterns similar in direction and tendency to those derived from ECG, indicating its potential utility in emotion monitoring.

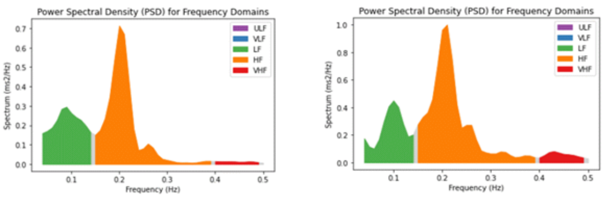

Fig. 11. HRV analysis during exposure to neutral visual stimuli (left: ECG-derived signal, right: textile sensor-derived signal)

Table 2. LF/HF ratio during exposure to emotionally neutral visual stimuli

	ECG signal	Textile sensor signal
LF/HF ratio	0.64579	0.321256

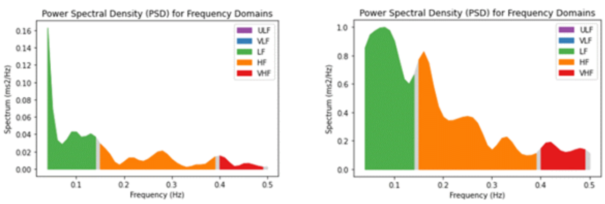

Fig. 12. HRV analysis during exposure to high-fear visual stimuli (left: ECG-derived signal, right: textile sensor-derived signal)

Table 3. LF/HF ratio during exposure to high-fear visual stimuli

	ECG signal	Textile sensor signal
LF/HF ratio	1.538189	1.265557

4. CONCLUSION

In this study, a coil-type textile sensor based on a time-varying magnetic field was developed to explore its feasibility in detecting cerebral blood flow (CBF) signals and evaluating emotional states, in addition to previously validated capabilities for cardiac and respiratory signal monitoring. When applied to the carotid artery region, the textile sensor exhibited signal patterns that varied in accordance with changes in blood flow velocity measured by Doppler ultrasonography, thereby verifying its potential for noncontact hemodynamic signal acquisition.

To assess emotional responses, heart rate variability (HRV) was extracted from ECG (R–R intervals) and textile sensor signals (peak-to-peak intervals from PLL output). Although the absolute HRV values differed slightly between the two modalities—partly due to the textile signal's susceptibility to noise and the absence of distinct R-peaks—their LF/HF ratio trends showed similar autonomic nervous system modulation in response to visual stimuli. These results support the applicability of the proposed textile sensor for emotion monitoring through indirect physiological markers.

Despite these promising outcomes, the study has several limitations. The sample size was small, and synchronization between the Doppler system and textile sensor was not possible due to hardware constraints. Moreover, the textile sensor's signal resolution, particularly under motion conditions, presents challenges for peak-based analysis. These limitations suggest the need for more robust signal processing and broader validation.

Future research should aim to refine the textile sensor's signal fidelity through improved coil design, noise filtering, and peak detection algorithms. Longitudinal studies with larger participant groups in real-world settings are also warranted. Furthermore, integrating the sensor into a fully wearable and wireless system could facilitate unobtrusive, real-time monitoring of physiological and emotional states in everyday environments—ultimately bridging the gap between lab-based assessments and ecological, user-centered affective computing.

5. REFERENCES

[1] J.E. Lee, S.K. Yoo, Feature Selection Classifier Design for Emotion Detection using Physiological Signals, J. Inst. Electron. Eng. Korea, 50(11) (2013) 2910 - 2920. https://doi.org/10.5573/ieek.2013.50.11.206

[2] M. Li, B.L. Lu, Emotion Classification Based on Gamma-band EEG, Proc. IEEE EMBS Annu. Int. Conf., (2009) 1323 - 1326, Minnesota, USA.

[3] F. Agrafioti, D. Hatzinakos, A.K. Anderson, ECG Pattern Analysis for Emotion Detection, IEEE Trans. Affect. Comput., 3(1) (2012) 102 - 115. https://doi.org/10.1109/T-AFFC.2011.28

[4] M. Murugappan, N. Ramachandran, Y. Sazali, Emotion Classification from EEG Using DWT, J. Biomed. Sci. Eng., 3(4) (2010) 390 - 396. https://doi.org/10.4236/jbise.2010.34054

[5] J.H. Kim, E. André, Emotion Recognition Based on Physiological Changes in Music Listening, IEEE

Trans. Pattern Anal. Mach. Intell., (2008) 2067 – 2083. https://doi.org/10.1109/TPAMI.2008.26
[6] W.Y. Cha, D.K. Shin, D.I. Shin, Analysis and Comparison of the Emotion Recognition by Multiple Bio-Signal, Korea Comput. Sci. Conf., 37(1) (2010) 104 – 105.
[7] B.J. Park, E.H. Jang, M.A. Chung, S.H. Kim, J.H. Sohn, Emotion Classification Using Physiological Signals, Ergonomics Soc. Korea Conf. Proc., (2012) 370 – 374.
[8] M.C. Whang, S.I. Park, Brain-Heart Neural Connectivity and Emotion, J. Arch. Inst. Korea, 58(9) (2014) 59 – 62.
[9] E.H. Jang, Y.J. Eum, S.H. Kim, J.H. Sohn, Discrimination of Three Emotions Using ANS Parameters, Ergonomics Soc. Korea Conf. Proc., (2011) 369 – 363.
[10] K.H. Chon, J.Y. Oh, S.H. Park, Y.M. Jeong, D.I. Yang, A Study on Algorithm of Emotion Analysis using EEG and HRV, J. Korean Soc. Comput. Inform., 15(10) (2010) 105 – 112. https://www.kci.go.kr/kciportal/ci/sereArticleSearch/ciSereArtiView.kci?sereArticleSearchBean.artiId=ART001490108
[11] J.Y. Park, J.H. Park, J.H. Park, D.S. Park, Human Sensibility Measurement by Bio-Signal Analysis, Proc. Korean Soc. Mech. Eng., (2003) 935 – 939.
[12] S.O. Gi, Y.J. Lee, H.R. Koo, S.A. Khang, H.J. Park, K.S. Kim, J.H. Lee, J.W. Lee, Effect of Shape Features of Textile Electrode on Non-contact Cardiac Activity Sensing, Trans. Korean Inst. Electr. Eng., 62(6) (2013) 803 – 810. https://doi.org/10.5370/KIEE.2013.62.6.803
[13] S.O. Gi, Y.J. Lee, H.R. Koo, S.A. Khang, K.N. Kim, S.J. Kang, J.H. Lee, J.W. Lee, Textile-Based Inductive Sensor for Vital Sign Monitoring, J. Electr. Eng. Technol., 10(1) (2015) 364 – 371. https://doi.org/10.5370/JEET.2015.10.1.364
[14] S.O. Gi, Y.J. Lee, H.R. Koo, S.P. Lee, K.H. Lee, K.N. Kim, S.J. Kang, J.H. Lee, J.W. Lee, Electrode Designs for Non-Contact Heart Activity Measurement, J. Med. Syst., 39 (2015) 191. https://doi.org/10.1007/s10916-015-0339-7
[15] H.R. Koo, Y.J. Lee, S.O. Gi, S.A. Khang, J.H. Lee, J.H. Lee, M.G. Lim, H.J. Park, J.W. Lee, Sensor Position Effects in Textile-Based Inductive Coil for HR Monitoring, J. Med. Syst., 38(2) (2014). https://doi.org/10.1007/s10916-013-0002-0
[16] H.R. Koo, Y.J. Lee, S.O. Gi, S.P. Lee, K.N. Kim, S.J. Kang, J.W. Lee, J.H. Lee, Module Design Effects for Garment-Type Heart Activity Monitoring, J. Korean Soc. Cloth. Text., 39(3) (2015) 369 – 378. https://doi.org/10.5850/JKSCT.2015.39.3.369
[17] H.R. Koo, J.W. Lee, J.H. Lee, Motion Artifact Reduction Module in Heart-Activity-Sensing Garments, Text. Res. J., 88(19) (2018) 2190 – 2205. https://doi.org/10.1177/0040517517716909
[18] S. Gabriel, R.W. Lau, C. Gabriel, The dielectric properties of biological tissues: III. Parametric models for the dielectric spectrum of tissues, Phys. Med. Biol., 41(11) (1996) 2271 – 2293. https://iopscience.iop.org/article/10.1088/0031-9155/41/11/003/pdf
[19] M. Steffen, A. Aleksandrowicz, S. Leonhardt, Mobile Noncontact Monitoring of Heart and Lung Activity, IEEE Trans. Biomed. Circuits Syst., 1(4) (2007) 250 – 257. https://doi.org/10.1109/TBCAS.2008.915633
[20] J. Vedru, R. Gordon, L.H. Humal, J. Trolla, Modeling of an Inductive Sensor of the Foucault Cardiogram, Estonian J. Eng., 17(3) (2011) 252 – 270. https://doi.org/10.3176/eng.2011.3.06
[21] J. Dillard, J. Anderson, The role of fear in persuasion, Psychol. Mark., 21 (2004) 909 – 926.
[22] A.T. Beck, N. Epstein, G. Brown, R. Steer, Beck Anxiety Inventory [Database record], APA PsycTests, 1988. https://doi.org/10.1037/t02025-000

ACKNOWLEDGEMENT

1. This research was supported by the National Research Foundation of Korea (NRF), funded by the Ministry of Science and ICT (MSIT) (No. 2RS-2023-NR076520).
2. This research was supported by a grant of the Korea Health Technology R&D Project through the Korea Health Industry Development Institute (KHIDI), funded by the Ministry of Health & Welfare, Republic of Korea (No. RS-2024-00438443).